2012

Mixed-valence state of symmetric diruthenium complexes: synthesis, characterization, and electron transfer investigation

DALTON TRANSACTIONS, CAMBRIDGE, v. 41, n. 48, pp. 14540-14546, NOV, 2012
http://www.producao.usp.br/handle/BDPI/42790

Dalton Transactions

Cite this: *Dalton Trans.*, 2012, **41**, 14540

www.rsc.org/dalton

PAPER

Mixed-valence state of symmetric diruthenium complexes: synthesis, characterization, and electron transfer investigation†

Solange de Oliveira Pinheiro,[a] Tércio de F. Paulo,[a,b] Dieric dos S. de Abreu,[a] Elisane Longhinotti,[c] Claudio H. B. Silva,[b] Gustavo F. S. Andrade,[d] Márcia L. A. Temperini[b] and Izaura Cirino Nogueira Diógenes*[a]

Received 1st March 2012, Accepted 26th September 2012
DOI: 10.1039/c2dt32092d

Complexes of the type $\{[(pyS)Ru(NH_3)_4]_2$-μ-L$\}^n$, where pyS = 4-mercaptopyridine, L = 4,4′-dithiodipyridine (pySSpy), pyrazine (pz) and 1,4-dicyanobenzene (DCB), and n = +4 and +5 for fully reduced and mixed-valence complexes, respectively, were synthesized and characterized. Electrochemical data showed that there is electron communication between the metal centers with comproportionation constants of 33.2, 1.30×10^8 and 5.56×10^5 for L = pySSpy, pz and DCB, respectively. It was also observed that the electronic coupling between the metal centers is affected by the π-back-bonding interaction toward the pyS ligand. Raman spectroscopy showed a dependence of the intensity of the vibrational modes on the exciting radiations giving support to the assignments of the electronic transitions. The degree of electron communication between the metal centers through the bridging ligands suggests that these systems can be molecular wire materials.

Introduction

Since the discovery of the Creutz–Taube mixed-valence complex,[1–3] $[(NH_3)_5Ru(\mu\text{-}pz)Ru(NH_3)_5]^{5+}$, where pz = pyrazine, more than four decades of experimental and theoretical investigation have been needed to reach some agreement on the delocalized nature of the electronic structure, and some observables still remain to be explained.[4–13] In addition, mixed-valence complexes have attracted a lot of attention due to the interest in the synthesis of the so-called molecular wires. These materials can be defined as "*a molecule between two reservoirs of electrons*" or "*a molecule that conducts electrical current between two electrodes*", according to Kirczenow[14] and Ratner,[15] respectively. Such systems have great promise from a pure science perspective and also potentially for applications. In fact, long-range electron transfer reactions are of great importance in almost all areas of chemistry ranging from biological chemistry to the synthesis of new materials for electronic devices.[15–17] As expected, the understanding of such systems has not been a simple matter. It is well known that several aspects such as separation between the redox centers and molecular conformation affect the electron transfer and most of the times it cannot be accurately known. Due to this, mixed-valence binuclear complexes have been used to investigate long-range electron transfer reactions[10,16,17] because in such compounds the electron transfer occurs within the molecule through a bridging ligand whose structure and conformation are known (at least in the ground state). In the context of molecular electronics owing to their potential application as molecular wires, the interest in the linear geometry has increased. As a consequence, the synthesis and characterization of several linear systems based on coordination complexes have been reported lately.[10,17–19] Focusing on the production of molecular wires, many synthetic approaches have tried to prepare oligonuclear transition metal complexes with different degrees of electronic coupling between their constituents; hence, their design relies on the known properties of binuclear complexes.

Among the techniques used to study mixed-valence complexes, resonance Raman experiments involving the near-infrared (NIR) metal-to-metal charge transfer (MMCT) electronic absorption band have been successfully used to determine the vibrations of the bridging ligand that clearly includes the MMCT transition.[6,20,21]

In this work, binuclear ion complexes of the type $\{[(pyS)Ru(NH_3)_4]_2$-μ-L$\}^{n+}$, where pyS = 4-mercaptopyridine and L = 4,4′-dithiodipyridine (pySSpy), pyrazine (pz) and 1,4-dicyanobenzene (DCB), were studied in the fully reduced state, n = 4, and after one electron oxidation, n = 5. Electrochemistry and NIR spectroscopy are presented in an attempt to determine the degree of electron communication between the metal centers. Raman spectra were acquired at different exciting radiations in order not only to support the metal-to-ligand charge-transfer (MLCT)

[a]*Departamento de Química Orgânica e Inorgânica, Universidade Federal do Ceará, Cx. Postal 6021, Fortaleza-CE, Brasil, CEP: 60455-970. E-mail: izaura@dqoi.ufc.br*
[b]*Instituto de Química, Universidade de São Paulo, Cx. Postal 26077, São Paulo-SP, Brasil, CEP: 05599-970*
[c]*Departamento de Química Analítica e Físico-Química, Universidade Federal do Ceará, Cx. Postal 6021, Fortaleza-CE, Brasil, CEP: 60455-960*
[d]*Departamento de Química, Universidade Federal de Juiz de Fora, Juiz de Fora, Minas Gerais, Brasil, CEP: 36036-900*
†Electronic supplementary information (ESI) available. See DOI: 10.1039/c2dt32092d

assignments but also to determine the vibrational modes involved in the MMCT transitions.

Experimental

Apparatus

Elemental analyses were done at the Microanalysis Laboratory at the Institute of Chemistry at São Paulo University. Electronic spectra in the Ultraviolet and Visible (UV-Vis) regions were acquired with a Hitachi model U-2000 spectrophotometer while those in the UV-Vis-NIR (near infrared) regions were taken on a Varian Cary 5000 spectrophotometer. The transmission infrared spectra of the compounds dispersed in KBr were obtained by using a Perkin-Elmer instrument model Spectrum 1000.

Raman spectra were obtained in three different configurations: (1) a Renishaw Raman imaging microscope system 3000 equipped with a CCD (charge-coupled device) detector, and an Olympus (BTH2) with a 50× objective to focus the laser beam on the sample for the exciting radiation at 632.8 from He–Ne (Coherent laser); (2) Raman spectra at 647.1, 568.2 and 488.0 nm (combined Ar^+ and Kr^+ ions laser, Coherent INNOVA 70C spectrum) were obtained using a Jobin-Yvon T64000 triple spectrometer, with a liquid nitrogen cooled CCD detector. The spectral resolution was 4 cm^{-1} and the laser power was kept under 15 mW. To avoid local heating, a homemade spinning cell was used. The band at 988 cm^{-1} of the Na_2SO_4 solid sample was used as an internal standard for intensity measurement; (3) Raman spectra at 1064 nm excitation radiation (Nd:YAG laser, Coherent Compass 1064-500N) were obtained using an FT-Raman Bruker RFS 100 spectrometer with a liquid nitrogen cooled Germanium detector. The use of the configurations for each purpose is discussed in the Results and discussion section.

Electrochemical experiments were performed on an Epsilon electrochemical analyzer (Bioanalytical Systems-BAS, West Lafayette, IN) at 25 ± 0.2 °C. A three-electrode glass cell with two platinum disks (0.126 cm^2 of geometrical area) as working and auxiliary electrodes was used in the characterization of the complexes. The non-aqueous experiments were carried out in acetonitrile containing 0.1 mol L^{-1} tetra-*n*-butylammonium perchlorate (tbap) as a supporting electrolyte and ferrocene as an internal reference. These measurements were referenced to an Ag/AgCl electrode which was prepared by immersion of an Ag wire in a saturated KCl solution for 1 h and then in a glass tube containing the same electrolyte supporting solution to avoid junction potential contributions. All the electrochemical data, unless specified, are cited against the Normal Hydrogen Electrode (NHE). To adjust the potentials to the NHE, the ferrocenium/ferrocene couple is assumed to lie at 0.69 *vs.* NHE in acetonitrile.[22] Spectroelectrochemical measurements were carried out in a thin layer cell with gold grid, gold wire and Ag/AgCl (BAS, 3.5 M KCl) as working, auxiliary and reference electrodes, respectively. An aqueous solution containing 0.1 mol L^{-1} CH_3COONa (pH = 3.0) was used as an electrolyte medium.

Chemicals

The water used throughout was purified from a Milli-Q water system (Millipore Co.). Organic solvents (Merck and Aldrich) of spectroscopic grade were used as received. 4-Mercaptopyridine (pyS), 4,4′-dithiodipyridine (pySSpy), pyrazine (pz) and 1,4-dicyanobenzene (DCB) species were purchased from Aldrich and used as received. KCl, NaOH, CF_3COOH, $K_2S_2O_8$ and K_2SO_4 from Aldrich, $BaSO_4$ (Riedel-de Haën) and Na_2SO_4 (Baker's analyzed CP) were used without further purification. Tetra-*n*-butylammonium perchlorate (tbap), from Aldrich, was recrystallized three times from ethyl acetate and dried under vacuum for 72 h. Acetonitrile (chromatographic grade, from Mallinckrodt) was dried over 4 Å molecular sieves for 72 h prior to use. All other chemicals were of at least reagent grade quality and were used as received.

The starting complexes $[RuCl(NH_3)_5]Cl$, *trans*-$[RuCl(SO_2)(NH_3)_4]Cl$, and *trans*-$[Ru(SO_4)(NH_3)_4(pyS)]Cl$ were synthesized according to the literature procedure.[23,24] *trans*-$[Ru(NH_3)_4(pyS)(L)](PF_6)_2$ type complexes, where L = pySSpy, pz and DCB, were synthesized according to the literature procedures for similar compounds.[25–27] Symmetric binuclear compounds of the type $\{[Ru(NH_3)_4(pyS)]_2\text{-}\mu\text{-}L\}(PF_6)_4$ were synthesized according to the literature procedures for similar compounds.[28,29] In brief, 0.329 mmol of $[Ru(SO_4)(NH_3)_4(pyS)]^+$ were dissolved in water containing zinc amalgam for 30 min under stirring and an argon atmosphere. After that, the resulting solution was transferred through a tube to a reaction flask containing 0.164 mmol of the bridging ligands pz, pySSpy (1 : 1, ethanol–water) and DCB (methanol) dissolved in a deaerated solvent (or in a mixture of solvents). The reaction solutions were kept under stirring and argon flux for 5 h when NH_4PF_6 was added. The precipitates were collected, redissolved in water and chromatographically purified (Bio-Gel P2). The mixed-valence species were generated from the reduced binuclear complexes either chemically or electrochemically. The chemical oxidation was performed with stoichiometric amounts of $K_2S_2O_8$, while the electrochemical oxidation was achieved by constant potential electrolysis and monitored by absorption spectroscopy. Whenever it was needed, the re-reduction was achieved by the addition of zinc amalgam.

The electrochemical characterizations were carried out employing cyclic voltammetry and differential pulse voltammetry techniques. All the synthesized compounds presented well-defined waves assigned to the $Ru^{III/II}$ redox process.[30] In such case, the formal potential (E') values were calculated as the average of anodic (E_{ap}) and cathodic (E_{cp}) peak potentials, $E' = (E_{ap} + E_{cp})/2$, in CV measurements.

***trans*-$[Ru(NH_3)_4(pyS)_2](PF_6)_2\cdot H_2O$.** Anal. calc.: C: 16.79; H: 3.38; N: 11.75; S: 8.96%. Found: C: 16.43; H: 3.24; N: 11.39; S: 8.49%. Yield: 76%. UV-Vis (H_2O) λ_{max} (MLCT transition) in nm (ε in L mol^{-1} cm^{-1}): 491(5.9×10^2). E' (CH_3CN) = 0.28 V *vs.* NHE.

***trans*-$[(pyS)Ru(NH_3)_4]_2\text{-}\mu\text{-}pySSpy)](PF_6)_4$.** Anal. calc.: C: 17.68; H: 2.97; N: 12.37; S: 9.44%. Found: C: 17.24; H: 2.87; N: 12.15; S: 9.06%. Yield: 52%. UV-Vis (CH_3CN) λ_{max} (MLCT transitions) in nm (ε in L mol^{-1} cm^{-1}): 472(17.0×10^3), 609(8.0×10^2). $E'(1)$ = 0.49 V *vs.* NHE, $E'(2)$ = 0.58 V *vs.* NHE (in CH_3CN).

***trans*-$[(pyS)Ru(NH_3)_4]_2\text{-}\mu\text{-}pz)](PF_6)_4$.** Anal. calc.: C: 13.80; H: 2.98; N: 13.79; S: 5.26%. Found: C: 13.52; H: 2.91; N: 13.57; S: 5.08%. Yield: 34%. UV-Vis (CH_3CN) λ_{max} (MLCT

transitions) in nm: 477(5.6 × 10^3), 589(3.3 × 10^3). $E'(1)$ = 0.23 V *vs.* NHE, $E'(2)$ = 0.72 V *vs.* NHE (in CH_3CN).

***trans*-[(pyS)Ru(NH$_3$)$_4$]$_2$-μ-DCB)](PF$_6$)$_4$·1.3H$_2$O.** Anal. calc.: C: 14.82; H: 2.63; N: 11.52; S: 4.40%. Found: C: 14.49; H: 2.63; N: 11.38; S: 4.26%. Yield: 66%. UV-Vis (CH_3CN) λ_{max} in nm (ε in L mol^{-1} cm^{-1}): 457(22.0 × 10^3), 613(2.0 × 10^2). $E'(1)$ = 0.85 V *vs.* NHE, $E'(2)$ = 1.19 V *vs.* NHE (in CH_3CN).

Results and discussion

Fully reduced binuclear complexes

Electronic spectra. The UV-Vis electronic spectra of the fully reduced binuclear complexes present two absorptions in the region from 450 to 680 nm, besides the intraligand transitions (from 200 to 400 nm). Because of the dependence of the energy on the solvent nature[31] (see Table S1 in the ESI† file), these absorptions were assigned to metal-to-ligand charge transfer (MLCT) transitions from the Ru(II) ions to terminal pyS and bridging ligands (pySSpy, pz and DCB). Based on the UV-Vis spectra of *trans*-[Ru(NH$_3$)$_4$(pyS)$_2$]$^{2+}$ and *trans*-[Ru(NH$_3$)$_4$(OH$_2$)-(pyS)]$^{2+}$ monomers (Experimental section), the absorptions observed at 472, 491 and 457 nm in the UV-Vis spectra of the binuclear complexes are assigned to the MLCT transitions to the pyS ligand, pyS(pπ*) ← (dπ)Ru^{II} while those at lower energies are assigned to the bridging ligand (Fig. 1, insets). These bands are observed at 609, 589 and 613 nm when pySSpy, pz and DCB are the bridging ligands, respectively.

Vibrational Raman spectra. It is well known that when the wavelength of the exciting radiation (λ_0) is close to the wavelength of an electronic transition of the sample, the intensities of the Raman bands of the molecular moiety involved in the electronic transition are strongly enhanced.[32] Aiming to support the assignments of the MLCT transitions of {[(pyS)Ru(NH$_3$)$_4$]$_2$-μ-L}(PF$_6$)$_4$ type complexes, Raman spectra were acquired by using 488.0, 568.2 and 647.1 nm as exciting lines and are illustrated in Fig. 1. For the acquisition of the Raman spectra, the solid samples were dispersed in $BaSO_4$ because this salt does not absorb any of the laser lines used in the resonance Raman experiments and it presents an intense band at 988 cm^{-1}, which was used as an internal standard band. The most prominent bands and their assignments as well as their relative intensities are displayed in Table 1.

Although all bridging and terminal ligands present a similar framework, a dependence of the relative intensity of some vibrational modes on the exciting radiations can be observed in the spectra displayed in Fig. 1, Table 1 and Table S2 of the ESI.†

The spectra at 647.1 nm present an enhancement of the bands at lower wavenumbers (from 250 to 460 cm^{-1}) for all the complexes. These bands are assigned[7,27,39–42] to skeletal vibrational modes involving stretching vibrations of Ru–N of the different ligands and bending (N–Ru–N) of the NH_3.

The coupling of the stretching vibrational mode of the C–S bond, ν(CS), with the 12a$_1$ ring breathing mode of 4-mercaptopyridine (pyS) Lewis base results in a signal at 1104 cm^{-1} known as X-sensitive band due to the sensitivity toward changes in the ring *trans* substituent.[33–38] Upon coordination to

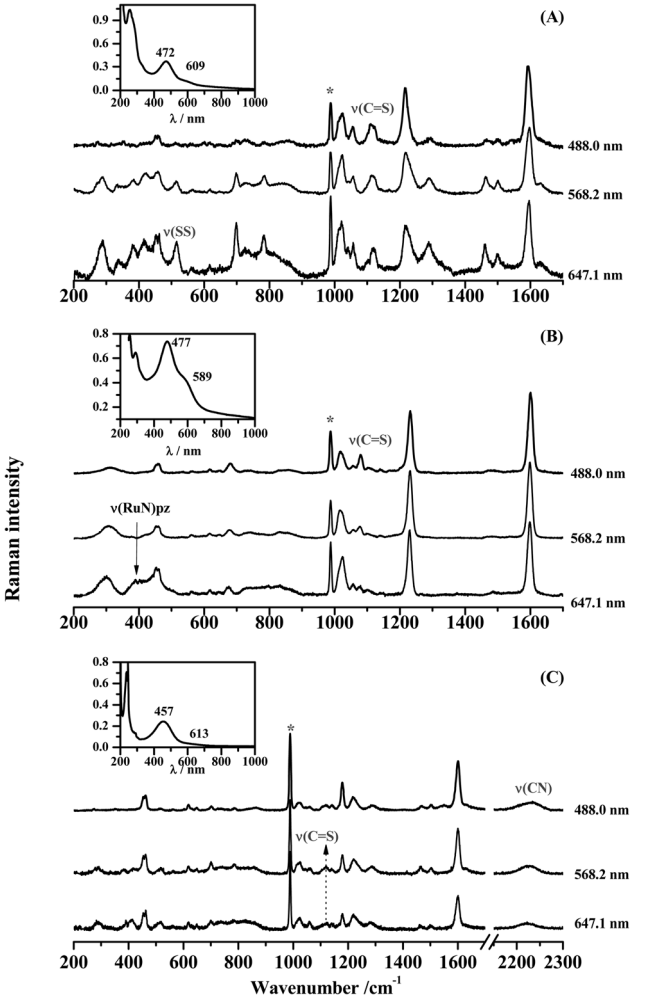

Fig. 1 Resonance Raman spectra of homogeneous solid mixtures of $BaSO_4$ with (a) {[(pyS)Ru(NH$_3$)$_4$]$_2$-μ-pySSpy}(PF$_6$)$_4$, (b) {[(pyS)Ru-(NH$_3$)$_4$]$_2$-μ-pz}(PF$_6$)$_4$ and (c) {[(pyS)Ru(NH$_3$)$_4$]$_2$-μ-DCB}(PF$_6$)$_4$ complexes at 647.1, 568.2 and 488.0 nm exciting radiations. Insets: UV-Vis spectra of the binuclear complexes in acetonitrile. (*) $BaSO_4$ band.

ruthenium metal centers in monomer complexes,[26,37,38] this mode shifts to *ca.* 1120 cm^{-1} indicating that the coordination does not occur *via* the sulfur atom as expected for pyridyl based ligands. In the binuclear complexes under study, this mode is observed at 1119, 1076 and 1123 cm^{-1} when the bridging ligands are pySSpy, pz and DCB, respectively. Apart from the {[(pyS)Ru(NH$_3$)$_4$]$_2$-μ-DCB}(PF$_6$)$_4$ complex in which the band at 1123 cm^{-1} showed no dependence on the exciting radiations, the relative intensities of these bands are enhanced at 488.0 nm. This result suggests that the absorptions observed from 450 to 480 nm in the UV-Vis spectra of these binuclear complexes (insets in Fig. 1) are, indeed, due to MLCT transitions to the pyS terminal ligand. On the other hand, the intensities of the bands at 515 and 390 cm^{-1} assigned, respectively, to the stretching vibrations of SS (pySSpy) and Ru–N (pz) bonds are enhanced at 647.1 nm meaning that the lower energy absorptions in the UV-Vis spectra are associated with MLCT transitions to pySSpy and pz bridging ligands. When DCB is the bridging ligand, although the ν(C≡N) mode is clearly observed at 2223 cm^{-1}

Table 1 Relative intensities of Raman bands of $\{[(pyS)Ru(NH_3)_4]_2$-μ-L$\}(PF_6)_4$ type complexes at different exciting radiations (λ_0). A more extensive assignment table is presented as Table S2 in ESI†

		Relative intensities λ_0/nm			
L	ν^a/cm^{-1}	647.1	568.2	488.0	Assignment[27,33–42]
	515	0.42	0.29	0.06	ν(SS) pySSpy
	698	0.67	0.49	0.13	δ(CCC) + ν (CS) pySSpy
	1021	0.69	0.93	0.72	1a ring breathing pySSpy + pyS
	1119	0.35	0.44	0.48	12a$_1$ ring breathing + ν (C═S) pyS
	1595	0.94	1.61	1.58	ν(CC) pyS
	390	0.29	0.00	0.00	ν(RuN) pz
	1024	0.72	0.74	0.52	1a ring breathing pz + pyS
	1076	0.16	0.31	0.44	12a$_1$ ring breathing pyS + ν(C═S) pyS
	1230	1.22	1.79	1.48	β(CH) pz + pyS
	1599	1.37	2.01	1.92	ν(CC) pz + pyS
	1023	0.14	0.15	0.10	1a ring breathing DCB + pyS
	1123	0.07	0.09	0.07	12a$_1$ ring breathing + ν(C═S) pyS
	1179	0.20	0.25	0.36	β(CH) DCB
	1600	0.42	0.61	0.64	ν(CC) DCB + pyS
	2223	0.07	0.11	0.11	ν(C≡N) DCB

[a] Frequencies related to spectra at 647.1 nm.

indicating the coordination of the ligand to the metal centers, the spectra analysis is not straightforward probably due to the very low intensity of the UV-Vis absorption at 613 nm (Fig. 1C, inset). In such case, the vibrational modes associated with the bridging ligand do not show significant changes in intensity by changing exciting lines thus not allowing a conclusive assignment.

Electrochemistry. In the absence of any metal–metal interaction, symmetric dimetallic complexes would exhibit metal-based oxidations at the same potential for both metal centers. The cyclic voltammograms of the studied binuclear complexes, however, presented two sequential one-electron reversible waves, assigned to the $Ru^{III/II}$ redox processes, indicating that there is communication across the bridging ligands.

The difference in potential ($\Delta E'$) between two pairs of waves in a binuclear compound depends not only on the interactions between the metals, but also on the change in electronic structure of the bridging ligand due to two bound metal centers. For the complexes presented in this study, these potentials would formally correspond to the following processes:

$$Ru^{II} - L - Ru^{II} \overset{E'(1)}{\rightleftharpoons} Ru^{II} - L - Ru^{III} \overset{E'(2)}{\rightleftharpoons} Ru^{III} - L - Ru^{III} \quad (1)$$

Table 2 presents the electrochemical data obtained for *trans*-$\{[(pyS)Ru(NH_3)_4]_2$-μ-L$\}^{4+}$ type complexes, where L = pz, pySSpy and DCB, as well as the values of comproportionation constants, K_C. Data for similar compounds are also presented for comparative purpose.

The value of $\Delta E'$ reflects the degree of electron delocalization, *i.e.* the greater the difference, the greater the electron communication between the metal centers.[43–45] This parameter allows, also, the evaluation of the stabilization or destabilization of the metal π orbitals (t_{2g}) by coordination to a second metal unit. Such change could be dictated by variations in the π-accepting ability of the bridge, which can be modulated by the size, degree of conjugation, and conformational aspects. Additionally, the comproportionation equilibrium constant, K_C, which reflects the equilibrium illustrated in eqn (2),

$$Ru^{II} - L - Ru^{II} + Ru^{III} - L - Ru^{III} \overset{K_C}{\rightleftharpoons} Ru^{II} - L - Ru^{III} \quad (2)$$

can be calculated based on the electrochemical results,[44] according to eqn (3):

$$K_C = \exp\left(\frac{[E'(2) - E'(1)](n_1 n_2)F}{RT}\right) \therefore \text{ at } T = 298.15\,\text{K}$$
$$\Rightarrow K_C = \exp(\Delta E'/25.69\,\text{mV}) \quad (3)$$

where n_1 and n_2 are the number of electrons of the electrode reactions and R, T, and F have their usual meaning.

The results displayed in Table 2 indicate that the higher electronic coupling is observed with pz as a bridging ligand, which is consistent with the shorter size and greater degree of conjugation of this moiety.

The effect of a competitive π-back-bonding interaction to the terminal ligand, pyS, can be seen by comparing the data acquired for pz and DCB when used as bridging ligands. The lower value of $\Delta E'$ observed for DCB indicates a decrease in the electronic coupling across the bridge as a consequence of an increase in the π-back-bonding interaction to pyS.

For $\{[(pyS)Ru(NH_3)_4]_2$-μ-pySSpy$\}^{4+}$, a different behavior is observed. We believe that, in such case, the electron delocalization toward the pyS ligand reduces the electron density on the SS bond of pySSpy resulting in the increase of flexibility which decreases the electronic coupling across the bridge. This can be noticed by the relatively lower value of the comproportionation constant (K_C = 33.2). In fact, when the terminal ligand is NH_3 instead of pyS, the value of K_C is 1.18×10^5 meaning that there is a meaningful electron coupling across the bridge.

Although the determination of the electron communication between two metal centers through a bridging ligand has been shown to be affected by aspects such as solvent and supporting electrolyte,[13,46] the values displayed in Table 2 indicate that the studied binuclear complexes belong to Class II, by considering the experimental conditions and in accordance with the Robin and Day classification.[47]

Mixed-valence complexes

Electronic spectroscopy. Following the addition of the $K_2S_2O_8$ oxidizing agent, the intensity of the MLCT absorptions in the UV-Vis spectra of the fully reduced complexes decreases while a new band appears in the near-IR (NIR) region. Once these complexes are fully oxidized, these absorptions disappear indicating the metal-to-metal charge transfer (MMCT) nature of the transition. To study this process, the mixed-valence complexes (one electron oxidized species) were generated by chemical oxidation, which was performed with the addition of stoichiometric amounts of $K_2S_2O_8$. The reversibility of the absorption bands was observed for all the compounds when one electron oxidized species were produced (Fig. S2 in the ESI† shows the spectra profile during electrolysis). Fig. 2 shows the

Table 2 Electrochemical data (V *vs.* NHE) in acetonitrile containing 0.1 mol L^{-1} tbap and K_C values of *trans*-$\{[(pyS)Ru(NH_3)_4]_2$-μ-L$\}^{4+}$ and *trans*-$\{[Ru(NH_3)_5]_2$-μ-L$\}^{4+}$ type complexes

Compound	$E'(1)$	$E'(2)$	$\Delta E'$	K_C	Reference
$\{[(pyS)Ru(NH_3)_4]_2$-μ-pz$\}^{4+}$ [a]	0.21	0.69	0.48	1.30×10^8	This work
$\{[(pyS)Ru(NH_3)_4]_2$-μ-pySSpy$\}^{4+}$ [a]	0.47	0.56	0.09	33.2	This work
$\{[(pyS)Ru(NH_3)_4]_2$-μ-DCB$\}^{4+}$ [b]	0.83	1.17	0.34	5.56×10^5	This work
Creutz–Taube ion	0.37	0.76	0.39	4.20×10^6	1
$\{[Ru(NH_3)_5]_2$-μ-pySSpy$\}^{4+}$	0.12	0.42	0.30	1.18×10^5 [c]	28

[a] Differential pulse voltammetry at 0.02 V s^{-1} and [b] cyclic voltammogram at 0.1 V s^{-1} (glassy carbon electrode). [c] A typo must be committed in ref. 28 for a value of 8×10^4 was reported based on equation $K_c = \exp(\Delta E_{1/2}/25.69\ mV)$.

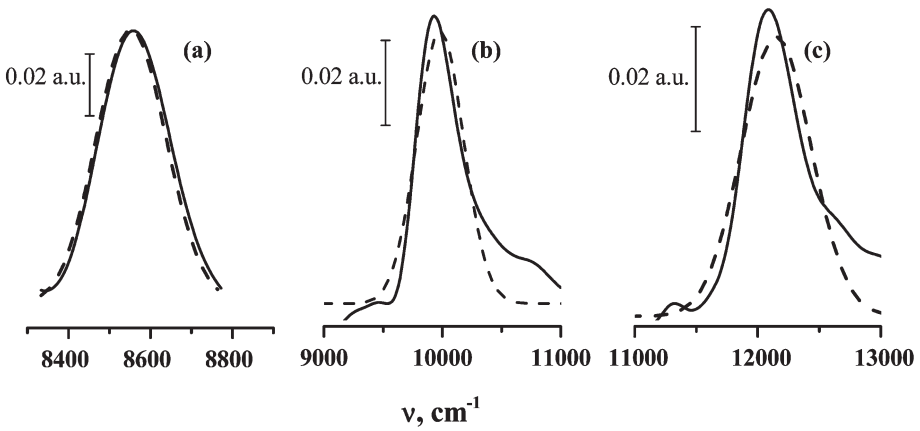

Fig. 2 NIR spectra of the mixed-valence compounds of the type $\{[(pyS)Ru^{III}(NH_3)_4$-L-$Ru^{II}(NH_3)_4(pyS)]\}^{5+}$ in acetonitrile, where L = pySSpy (a), pz (b) and DCB (c). Dotted lines correspond to Gaussian fits to the experimental bands.

Table 3 Spectroscopic data obtained from the deconvoluted spectra of the mixed-valence compounds of the type $\{[(pyS)Ru^{III}(NH_3)_4$-μ-L-$Ru^{II}(NH_3)_4(pyS)]\}^{5+}$ in acetonitrile

L	λ_{max} (nm), ε_{max}, (mol^{-1} L cm^{-1})	ν_{max} (cm^{-1})	E_{op}, eV	$\Delta\nu_{1/2\ max}$ (cm^{-1}) (exp.)	$\Delta\nu_{1/2\ max}$ (cm^{-1}) (calc.)	r_{MM} [a], Å	H_{AB} (cm^{-1})	α
pySSpy	1173 (700)	8525	1.06	197.90	4437.65	7.50	230	0.10
pz	1004 (915)	9960	1.23	423.82	4796.62	6.80	302	0.19
DCB	826 (850)	12 100	1.50	616.82	5286.87	11.80	270	0.13
pz [b]	1570 (3000)	6369	0.78	1400.00	—	6.80	3300	0.48
pySSpy [b]	1500 (1500)	6666	0.82	4300.00	—	7.50	855	0.12

[a] Distance between the metal centers, ref. 8, 48 and 49. [b] Complexes of the type *trans*-$\{[Ru^{II}(NH_3)_5]$-μ-L-$[Ru^{III}(NH_3)_5]\}$, ref. 8 and 50.

NIR spectra of the mixed-valence compounds in the region of the MMCT transition. The spectroscopic data obtained from these spectra are summarized in Table 3.

The values of the electronic coupling parameter (H_{ab}), which is important for understanding how efficiently the electron delocalization occurs through the bridge, indicate that the pz ligand shows more effective coupling than the other complexes under study. In comparison to the values reported[8,50] for $\{[Ru^{II}(NH_3)_5]$-μ-L-$[Ru^{III}(NH_3)_5]\}$ type complexes, the obtained data are lower being consistent with the presence of a π withdrawing ligand, pyS. One can conclude, therefore, that the competition for the electron density of the metal centers should be taken into account as previously commented.

The values of the full width of the band at half-height, $\Delta\nu_{1/2}$, are smaller than those calculated based on the theoretical expression of Hush[51,52] $\Delta\nu_{1/2} = 2310\nu_{max}$ (at 298 K), where ν_{max} is the maximum absorption energy in cm^{-1}. This observation suggests that the mixed-valence complexes studied in this work can be assigned to a Class III regime while the values of α are within $0 < \alpha < 0.70$ suggesting Class II as indicated based on electrochemical data. In addition, the dependence of the transition energy (E_{op}) on the solvent nature, which is displayed in Table 4, also suggests a Class II regime. This apparent discrepancy suggests that these compounds may be on the borderline between Class II and Class II–III regimes. For each mixed-valence ion, the plots of E_{op} *vs.* $(1/\eta^2 - 1/D_S)$, where η and nD_S are the optical and dielectric constants of the solvent, respectively, were observed to be linear as predicted[51,52] for a Class II regime (see Fig. S4† for the plots of E_{op} *vs.* $[(1/\eta^2) - (1/D_S)]$ in different solvents). The data were fitted using a linear least-

Table 4 Values of E_{op} in different solvents for the synthesized $\{[(pyS)Ru^{III}(NH_3)_4\text{-}\mu\text{-}L\text{-}Ru^{II}(NH_3)_4(pyS)]\}^{5+}$ complexes

	E_{op} (cm^{-1})			
L	Acetone	Acetonitrile	DMSO	D_2O
pySSpy	9937	8525	8505	7589
DCB	8511	12 100	10 224	10 739
pz	9297	9960	7897	7954

squares calculation and the correlation coefficients were between 0.9878 and 0.9925. The values of D_2O and DMSO are slightly off the line for L = pz and DCB, respectively. For D_2O and H_2O, specific interactions with the complexes have been noted previously[42,53,54] when bpy is the bridging ligand. In such case, the deviations may reflect the ability of these molecules to penetrate the planar bpy ligands turning the dielectric continuum approach used to predict the linear relation not fully appropriate. For the studied complexes, although this effect might be taken into account, the MMCT bands are not essentially Gaussian due to a shoulder at lower energies meaning that more than one band can exist. This distortion may affect the expected linear relation between E_{op} and $(1/\eta^2 - 1/D_S)$.

Raman spectroscopy. Fig. 3 shows the Raman spectra of the mixed-valence complexes at 632.8 and 1064 nm. The solid samples were dispersed in Na_2SO_4 salt, which was used as an internal standard to allow the analysis of the relative band intensities.

There is an expectation in this experiment in measuring the coupling of bridge motions to the MMCT transition. In such case, the intensity of the vibrational modes of the bridging ligands can be intensified at exciting radiations within or near the range of absorption of the MMCT absorption. For the mixed complexes under study, the maxima of these absorptions are observed at 1173, 826 and 1004 nm when the bridging ligands are pySSpy, DCB and pz, respectively (see Fig. 2). Therefore, 1064 and 632.8 nm are reasonable exciting lines to evaluate the effects of the near resonance (1064 nm) and non-resonance (632.8 nm) radiations on the vibrational modes of the bridging ligands.

All the spectra obtained at 1064 nm presented an intensification of the band at *c.a.* 280 cm^{-1} in comparison to those acquired at 632.8 nm. This band is assigned[7,27,39–42] to vibrational modes associated with Ru–N bonding in which ruthenium is bonded to NH_3 and/or pyridine ligands. In addition, as already commented, the skeletal vibrational modes of the complexes are observed in the region from 250 to 460 cm^{-1} in the Raman spectra of the fully reduced compounds.

The bands assigned to the S–S, C≡N and the ring breathing modes of the complexes in which the bridging ligands are, respectively, pySSpy, DCB and pz, are observed at 559, 2218 and 1023 cm^{-1} in the spectra at 1064 nm while in the spectra at 632.8 nm the S–S and C≡N modes are not detected. This observation indicates that these modes are clearly involved in the MMCT transition. In the case of the pz bridging ligand, the assignment is not straightforward since the band at 1023 cm^{-1} also contains vibrational modes of the terminal ligand, pyS. However, for the fully reduced complex (Table 1), this band is not intensified at 488 nm which coincides with the maximum of the MLCT transition to pyS meaning that, for the $\{[(pyS)\text{-}Ru^{III}(NH_3)_4\text{-}\mu\text{-}pz\text{-}Ru^{II}(NH_3)_4(pyS)]\}^{5+}$ ion complex, the band at 1023 cm^{-1} is mostly associated with the pz bridging ligand.

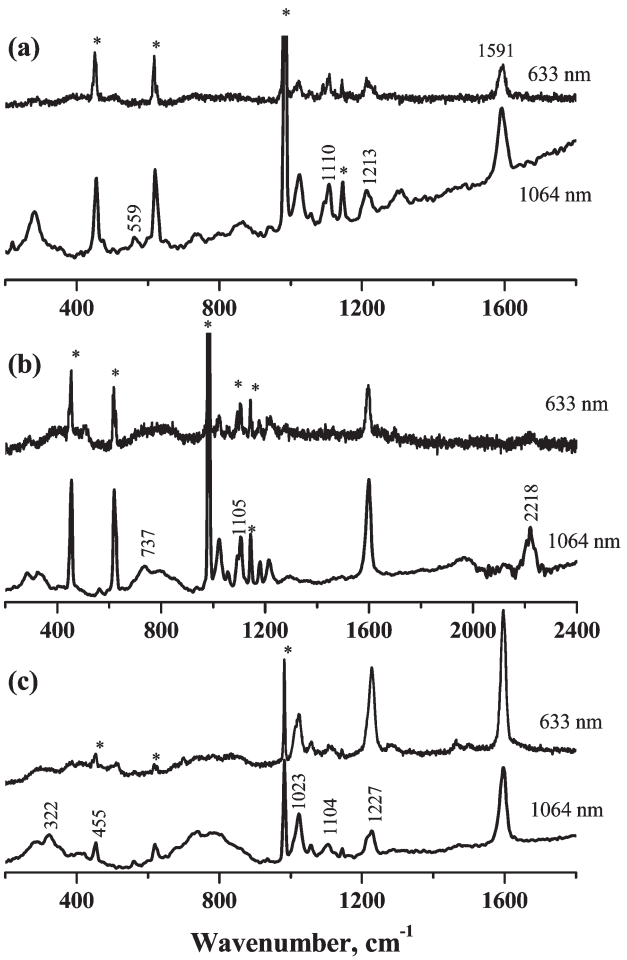

Fig. 3 Raman spectra at different exciting radiations of the mixed-valence complexes in which pySSpy (a), DCB (b) and pz (c) are the bridging ligands. *Na_2SO_4 bands.

Conclusion

A series of symmetric binuclear complexes of Ru was synthesized and characterized by electrochemistry and spectroscopic techniques. It was shown that the complexes of the type $\{[(pyS)Ru(NH_3)_4]_2\text{-}\mu\text{-}L\}^{n+}$, where L = pySSpy, pz and DCB, present electron communication between the metal centers where pz was the most effective bridge. Raman spectroscopy was used at different exciting radiations in order to support the assignments of the MLCT transitions of the fully reduced binuclear compounds. For the mixed-valence complexes, the NIR and Raman spectroscopies showed the MMCT transition parameters and the effect of this process on specific vibrational modes of the bridging ligands, respectively. Most of the results indicate that a Class II regime can be assigned to the studied compounds although a comparison between experimental and theoretical

values of the full width of the band at half-height suggests a Class III regime.

The results all together indicated that the degree of electron communication between the metal centers yields high delocalization through the bridging ligands being indicative that these systems can be molecular wire materials. However, π-back-bonding interaction must be taken into account since the positive effect of decreasing the band gap can be counterbalanced by the competition for the metal electron density between bridging and terminal ligands.

Acknowledgements

Temperini, M. L. A., Longhinotti, E. and Diógenes, I. C. N. are thankful to CNPq for the grants and FAPESP, FUNCAP (PRONEM PRN-0040-00065.01.00/10 SPU no.: 10582696-0) and CAPES for the financial support. Paulo, T. F. is thankful for the grant from FAPESP.

References

1 C. Creutz and H. Taube, *J. Am. Chem. Soc.*, 1969, **91**, 3988.
2 C. Creutz and H. Taube, *J. Am. Chem. Soc.*, 1973, **95**, 1086.
3 C. Creutz, *Prog. Inorg. Chem.*, 1983, **30**, 1.
4 J. T. Hupp, in *Comprehensive Coordination Chemistry II*, ed. J. McCleverty and T. J. Meyer, Elsevier, Amsterdam, 2004, vol. 2 (ed. A. B. P. Leve), p. 709.
5 K. D. Demadis, C. M. Hartshorn and T. J. Meyer, *Chem. Rev.*, 2001, **101**, 2655.
6 H. Lu and V. J. T. Hupp, *Chem. Phys. Lett.*, 1995, **235**, 521.
7 U. Furholz, H. B. Burgi, F. E. Wagner, A. Stebler, J. H. Ammeter, E. Krausz, R. J. H. Clark, M. J. Stead and A. Ludi, *J. Am. Chem. Soc.*, 1984, **106**, 121.
8 A. J. Distefano, J. F. Wishart and S. S. Isied, *Coord. Chem. Rev.*, 2005, **249**, 507.
9 P. V. Bernhardt, F. Bozoglián, B. P. Macpherson and M. Martinéz, *Coord. Chem. Rev.*, 2005, **249**, 1902.
10 W. Kaim and G. K. Lahiri, *Angew. Chem., Int. Ed.*, 2007, **46**, 1778.
11 P. Alborés, L. D. Slep, L. S. Eberlin, Y. E. Corilo, M. N. Eberlin, G. Benítez, M. E. Vela, R. C. Salvarezza and L. M. Baraldo, *Inorg. Chem.*, 2009, **48**, 11226.
12 S. D. Glover, J. C. Goeltz, B. J. Lear and C. P. Kubiak, *Coord. Chem. Rev.*, 2010, **254**, 331.
13 N. Vilà, Y.-W. Zhong, J. C. Henderson and H. D. Abruña, *Inorg. Chem.*, 2010, **49**, 796.
14 E. G. Emberly and G. Kirczenow, *Phys. Rev. B: Condens. Matter*, 1998, **58**, 10911.
15 A. Aviram and M. A. Ratner, *Chem. Phys. Lett.*, 1974, **29**, 277.
16 D. M. D'Alessando and F. R. Keene, *Chem. Rev.*, 2006, **106**, 2270.
17 F. Paul and C. Lapinte, *Coord. Chem. Rev.*, 1998, **180**, 431.
18 M. A. S. Silva, T. F. Paulo, S. O. Pinheiro, A. A. Batista, J. Ellena, E. H. S. Sousa, L. G. F. Lopes and I. C. N. Diógenes, *Polyhedron*, 2011, **30**, 2083.
19 F. Loiseau, F. Nastasi, A. M. Stadler, S. Campagna and J. M. Lehn, *Angew. Chem., Int. Ed.*, 2007, **46**, 6144.
20 C. H. Londergan, R. C. Rocha, M. G. Brown, A. P. Shreve and C. P. Kubiak, *J. Am. Chem. Soc.*, 2003, **125**, 13912.
21 R. C. Rocha, M. G. Brown, C. H. Londergan, J. C. Salsman, C. P. Kubiak and A. P. Shreve, *J. Phys. Chem. A*, 2005, **109**, 9006.
22 W. C. Barrette Jr., H. W. Johnson Jr. and D. T. Sawyer, *Anal. Chem.*, 1984, **56**, 1890.
23 L. H. Vogt Jr., J. L. Katz and S. E. Wiberley, *Inorg. Chem.*, 1965, **4**, 1157.
24 S. S. Isied and H. Taube, *Inorg. Chem.*, 1974, **13**, 1545.
25 E. Tfouni and P. C. Ford, *Inorg. Chem.*, 1980, **19**, 72.
26 S. O. Pinheiro, T. F. Paulo, M. A. S. Silva, G. F. S. Andrade, M. L. A. Temperini, I. M. M. Carvalho, J. R. Sousa, L. G. F. Lopes, F. A. Dias-Filho, E. H. S. Sousa, E. Longhinotti, M. O. Santiago, I. S. Moreira and I. C. N. Diógenes, *J. Braz. Chem. Soc.*, 2010, **21**, 1283.
27 H.-Y. Huang, W.-J. Chen, C.-C. Yang and A. Yeh, *Inorg. Chem.*, 1991, **30**, 1862.
28 I. S. Moreira and D. W. Franco, *Inorg. Chem.*, 1994, **33**, 1607.
29 J. E. Sutton, H. Krentzien and H. Taube, *Inorg. Chem.*, 1982, **21**, 2842.
30 A. J. Bard and L. R. Faulkner, in *Electrochemical Methods, Fundamentals and Applications*, John Wiley & Sons, New York, 1980.
31 A. B. P. Lever, in *Inorganic Electronic Spectroscopy*, Elsevier, Amsterdam, 1984.
32 R. J. H. Clark and T. Dines, *J. Angew. Chem., Int. Ed.*, 1986, **25**, 131.
33 J. Baldwin, N. Schuler, I. S. Butler and M. P. Andrews, *Langmuir*, 1996, **12**, 6389.
34 M. A. Bryant, S. L. Joa and J. E. Pemberton, *Langmuir*, 1992, **8**, 753.
35 H. T. Joo, M. S. Kim and K. Kim, *J. Raman Spectrosc.*, 1987, **18**, 57.
36 E. Spinner, *J. Chem. Soc.*, 1960, 1237.
37 I. C. N. Diógenes, F. C. Nart, M. L. A. Temperini and I. S. Moreira, *Inorg. Chem.*, 1999, **38**, 1646.
38 I. C. N. Diógenes, F. C. Nart, M. L. A. Temperini and I. S. Moreira, *Inorg. Chem.*, 2001, **40**, 4884.
39 H. I. S. Nogueira, S. M. G. Cruz, P. C. R. Soares-Santos, P. J. A. Ribeiro-Claro and T. Trindade, *J. Raman Spectrosc.*, 2003, **34**, 350.
40 K. Nakamoto, in *Infrared and Raman Spectra of Inorganic and Coordination Compounds*, Wiley, New York, 3rd edn, 1978.
41 V. Petrov, J. T. Hupp, C. Mottley and L. C. Mann, *J. Am. Chem. Soc.*, 1994, **116**, 2171.
42 R. W. Callahan, R. R. Keene, T. J. Meyer and D. J. Salmon, *J. Am. Chem. Soc.*, 1977, **99**, 1064.
43 J. E. Sutton and H. Taube, *Inorg. Chem.*, 1981, **20**, 3126.
44 J. E. Sutton, P. M. Sutton and H. Taube, *Inorg. Chem.*, 1979, **18**, 1017.
45 S. Flores-Torres, G. R. Hutchison, L. J. Soltzberg and H. D. Abruña, *J. Am. Chem. Soc.*, 2006, **128**, 1513.
46 B. D. Yeomans, L. S. Kelso, P. A. Tregloan and F. R. Keene, *Eur. J. Inorg. Chem.*, 2001, 239.
47 M. B. Robin and P. Day, *Adv. Inorg. Chem. Radiochem.*, 1967, **10**, 247.
48 T. Togano, H. Kuroda, N. Nagao, Y. Maekawa, H. Nishimura, F. S. Howell and M. Mukaida, *Inorg. Chim. Acta*, 1992, **196**, 57.
49 R. S. Nicholson and R. S. Shain, *Anal. Chem.*, 1964, **36**, 706.
50 W. C. Silva, J. B. Lima, I. S. Moreira, A. M. Neto, F. C. G. Gandra, A. G. Ferreira, B. R. McGarvey and D. W. Franco, *Inorg. Chem.*, 2003, **42**, 6898.
51 N. S. Hush, *Prog. Inorg. Chem.*, 1967, **8**, 391.
52 N. S. Hush, *Electrochim. Acta*, 1968, **13**, 1005.
53 R. W. Callahan and T. J. Meyer, *Chem. Phys. Lett.*, 1976, **39**, 82.
54 G. N. La-Mar and G. R. Van-Hecke, *Inorg. Chem.*, 1973, **12**, 1767.

